PROCEEDINGS OF SCIENCE

Starburst/AGN discrimination from combined MERLIN and VLA imaging of the 13hr deep survey

A. Zoghbi[*,1,2], **I. M^{c}Hardy**[1], **T. Dwelly**[1], **N. Seymour**[3], **D. Moss**[1], **T. Muxlow**[4], **R. Beswick**[4], **M. Page**[5], **N. Loaring**[6]

[*] *E-mail:* azoghbi@ast.cam.ac.uk

[1] *Department of Physics and Astronomy, University of Southampton, SO17 1BJ.*

[2] *Institute of Astronomy, Madingley Road, Cambridge CB3 0HA*

[3] *Spitzer Science Center, Caltech, 1200 East California Boulevard, Pasadena, CA 91125, USA.*

[4] *Nuffield Radio Astronomy Observatory, Jodrell Bank*

[5] *Mullard Space Science Laboratory, UCL, Holmbury St. Marry, Dorking, Surrey, RH5 6NT, UK*

[6] *SALT, PO box 9, Observatory, 7925, South Africa*

Using high resolution radio observations from the MERLIN, combined with a deep VLA observation of the 13hr field (13^h 34^m 37^s) , we were able to use morphology to discriminate between faint sources powered by AGN form those powered by star formation. This is important in order to understand the radio source count (at 1.4 GHz), and also, it can provide an independent measure of the star formation rates in the universe which is not effected by dust obscuration. Noise levels achieved were 18 μJy in the MERLIN maps, and 12 μJy in the combined (MERLIN + VLA) maps. We find that the contribution from star forming galaxies (SFG) increases significantly below 1 mJy, and that they contribute at least 60% to the faint radio population at around 100 μJy .

From planets to dark energy: the modern radio universe
October 1-5 2007
University of Manchester, Manchester, UK

PoS(MRU)117

1. Introduction

It has been established over the last few years by numerous measurments, that the global co-moving star formation rate (SFR) increases by an order of magnitude from $z = 0$ to $z = 1$ (Lilly et al. 1996; Madeau et al. 1996; Hammer et al. 1997; Wilson et al. 2002; Hopkins et al. 2004). For higher redshifts ($z > 2$), it was initially observed (Madeau et al. 1996) that the SFR decreases with redshift. However, later dust-corrected observations have shown that the rate may be flat up to redshift $z \sim 6$ (Hopkins et al. 2004).

The difficulty in measuring the SFR at high redshift is mainly due to dust-obscuration and the uncertainty in the correction which must be applied, which affects the implied galaxy luminosity at UV wavelengths.

The star formation rate can be detemined *independently* using radio observations. Radiation at radio wavelengths is known not to be affected by dust obscuration. The well-established radio-IR correlation (Helou et al. 1985) can be used to calculate the star formation rate from radio luminosities.

Radio surveys are dominated at high fluxes by AGN-powered sources. At fainter fluxes (below 1 mJy at 1.4GHz), radio surveys show an upturn in the Euclidean-normalised differential source counts. It has been suggested that this upturn results from the emergence of a new population of low luminosity radio sources powered by star formation (e.g. Richards 2000; Hopkins et al. 2003; Seymour et al. 2004). However the exact breakdown of the faint source population between AGN and starforming galaxies still remains largely unknown. Distinguishing between sources powered by AGN activity from those powered by star formation, is a vital step towards not just understanding the source counts, but also in determining the star formation history of the universe.

In this work, we present the classification of the a well-defined set of radio sources based on their radio morphology. High luminosity AGN show lobe-like structure which is extended well beyond the host galaxy, but there are very few such objects in the small areas covered by most radio deep surveys. In deep radio surveys AGN are most likely to be (flat spectrum) point sources coincident with the black hole in the nucleus of an optical galaxy. Radio emission in star forming galaxies, arising from, eg, extended supernovae activity is, on the other hand, often of low surface brightness, extended over all of the optical host galaxy. Such emission can be resolved-out in high resolution imaging and so may not be detected.

2. Observation & Analysis

The XMM-Newton/Chandra deep deep survey field centred at $13^h\ 34^m\ 37^s$, 37^o 54' 44" (13h field) with 15 arcmin radius was observed with the VLA at 1.4 GHz. The results were presented in Seymour et al. 2004 where 449 sources were detected down to a 4σ flux limit of 30 μJy (See Seymour et al. 2004 for details).

This field was also observed with the Multi-Element Radio-Linked Interferometer Array (MERLIN). The MERLIN observations were also carried out at 1.4 GHz. Because of the small primary beam (field of view) of MERLIN, four pointings were made, each covering about 10 arcmin diameter, to cover the deepest part of the VLA field. Each pointing lasted for 4 days giving a total of 16 days of observation.

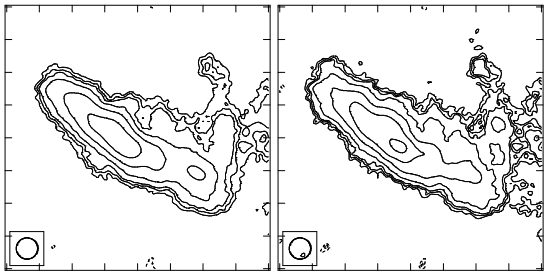

(a) map-plane combination

(b) UV-plane combination

Figure 1: Contour plots of a source made with the different methods of combination, contour levels are 3,4,5,8,16,32,64,128,256,512 times 18 μJy

The data were calibrated using the standard MERLIN analysis pipeline. Given the large computational requirements for imaging the full MERLIN primary beam in one map, we made small 'postage-stamp' maps centred on the positions of known 1.4GHz sources with total fluxes above 72 μJy , selected from the original VLA catalogue (Seymour et al. 2004). We further selected sources within 5 arcmin of the MERLIN pointing centre [1]. In total 127 VLA sources were mapped. The resulting natural weight maps had a resolution of 0.3 arcsec and typical RMS noise level of 18 μJy beam^{-1}. Fifty MERLIN sources (40%) showed the presence of a compact component at the position of the VLA source. For the remaining 77 VLA sources, there was no significant MERLIN detection.

To investigate the source morphologies further, the MERLIN and VLA datasets were combined. This combination results in maps with resolution and sensitivity which is intermediate between that of the separate VLA and MERLIN images. The data can be combined either in the map plane (eg see Muxlow et al. 2005) or in the UV-plane. Both methods were explored and figure 1 shows contour plots of the same source, made from the combined datasets, using the two different methods. There isn't much difference. In general, however, we preferred the UV-combination method as it allows for better removal of sidelobes from brighter sources, and better control on the quality and properties of the final combined maps (e.g tapering).

The combination of the two UV datasets, which have different channel numbers and different channel widths, was carried out as follows. Each dataset was first separated into single channels using the task SPLIT in the software package AIPS. Then, using the task DBCON, the individual channels were recombined into a single channel by recalculating the baseline lengths relative to the frequency of the first channel. The resulting two single-channel datasets (VLA and MERLIN) were then again combined using DBCON to produce a final single channel dataset. This dataset was used to produce images for the 127 selected sources. The final combined maps have a resolution fo 0.65 arcsec and a noise level of 12 μJy , which is intermediate between the MERLIN 18

[1] We limit the study to 5 arcmin to account for the shape of the primary beam. This was calculated by comparing fluxes of the point sources in the MERLIN to that of the VLA (which are expected to be the same). This resulted in a small correction of a factor of ~ 1.3 at a distance of 5 arcmin from the pointing centre.

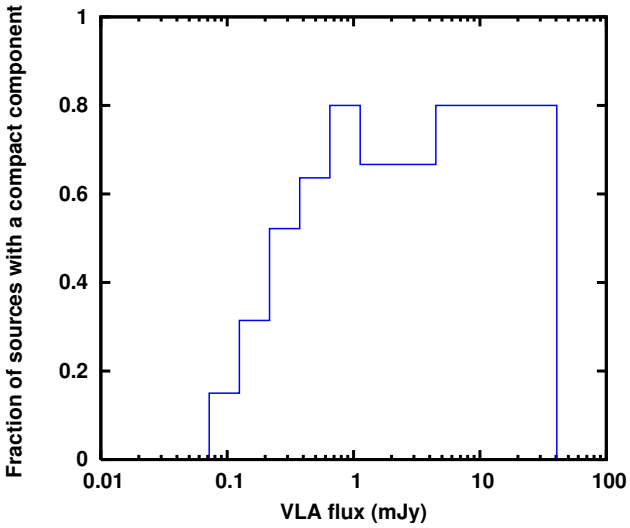

Figure 2: The fraction of sources with a compact component detected by MERLIN at the position of the VLA source as a function of VLA total flux.

μJy and the VLA 7.5 μJy noise levels.

3. Results & Discussion

Considering the MERLIN-only data with 0.3 arcsec resolution, in 40% of the sources a compact unresolved point source was detected, coinciding in almost all cases with centre of the optical galaxy. Although the upper limits on the sizes of the unresolved components were, in most cases, too large to determine a brightness temperature high enough to confirm an AGN (ie $> 10^5$K), the presence of unresolved nuclear sources is a strong indication that the source is powered by an AGN. On the other hand, bright VLA sources which are completely resolved out by MERLIN are probably starforming galaxies.

Figure 2 is a plot of the fraction of the number of VLA sources with a compact component detected by MERLIN as a function of the total VLA flux (from Seymour et al. 2004). The plot shows a decrease in the fraction of sources with a point-like core as the flux decreases. At the high flux end most of the sources (80%) are unresolved (or contain an unresolved component), while at the lower flux end only around 20% have a detectable compact component. At first sight figure 2 indicates a decreasing fraction of AGN as the total flux decreases. However if the sample contains some AGN where small-scale extended structure contains a noticeable fraction of the total VLA flux, then any unresolved core may be below the MERLIN sensitivity limit. If such AGN are of high luminosity where the extended emission is beyond the optical host galaxy, then they would have to be a very high redshifts and there are likely to be very few such objects in a deep survey such as ours. A more likely possibility is that the AGN itself lies in a galaxy with starburst emission extended on the scale of the galaxy. In that case figure 2 would tell us that the fraction of radio emission attributable to starbursts increases with decreasing radio flux.

In order to improve our search for extended low brightness emission we have examined the combined MERLIN and VLA maps. In these maps some of the sources that were not detected in

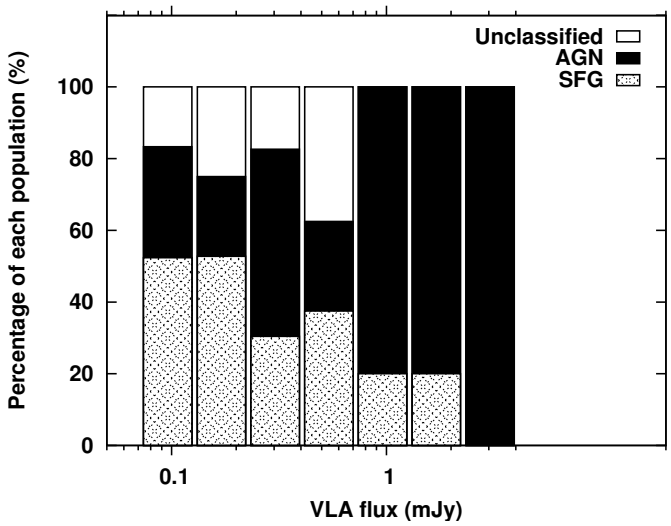

Figure 3: Percentage of sources in each population: A clear decrease in the contribution of AGN to the source numbers at lower fluxes, where Star Forming Galaxies SFG becomes more significant.

the MERLIN maps (to the 4σ level) showed some extended low brightness structure. The sources with compact components in the MERLIN maps alone still showed compact components in the combined maps. Using the information provided by the combined data and the original MERLIN maps, the sources were grouped individually into three classes: AGN, star forming galaxies (SFGs) and Unclassified using the flowing criteria:

- Sources with unresolved point-like structures in both maps (MERLIN and combined), at the centre of the host optical galaxy (if identifed), or without any optical counterparts, are classified as AGN.
- Sources showing jet-like structures are classified as AGN, particularly if an unresolved component is present.
- Sources with no MERLIN detection that show extended emission in the combined maps on the scale of the underlying galaxy are SFGs.
- Sources with unclear structures, or a combination of unresolved core emission with extended emission that does not clearly arise from a jet, are considered Unclassified.

The results of this classification are shown in figure 3, which again shows that the fraction of AGN becomes smaller at lower fluxes, while the percentage of star forming galaxies (SFG) increases below 1mJy. The fraction of unclassified sources also increases, not unexpectedly, below 1mJy. From the way 'unclassified' was defined earlier, these sources may contain a combination of emission from AGN and SFGs.

We conclude that, on the basis of their radio morphologies, AGN dominate deep radio surveys above flux levels of about 1mJy. However the fraction of star forming galaxies, or galaxies where starformation contributes a major fraction of the radio luminosity, increases as we go to fainter flux levels and constitue at least $\sim 60\%$ of the population of faint radio sources at about 100 μJy .

References

[1] Helou G., Soifer B, T., Rowan-Robinson M, *Thermal infrared and nonthermal radio - Remarkable correlation in disks of galaxies*, *ApJL*,**289, L7** (1985).

[2] Hammer, F., et al., *Canada-France Redshift Survey. XIV. Spectral Properties of Field Galaxies up to* $z = 1$, *ApJ*, **481, 49** (1997).

[3] Hopkins A. M., Afonso J., Chan B., Cram L. E., Georgakakis A., Mobasher B, *The Phoenix Deep Survey: The 1.4 GHz Microjansky Catalog*, *AJ*, **125, 465** (2003).

[4] Hopkins A. M, *On the evolution of star-forming galaxies*, *ApJ*,**615, 209**(2004).

[5] Lilly S. J., Fevre O. L., Hammer F., Crampton D, *The Canada-France Redshift Survey: The Luminosity Density and Star Formation History of the Universe to Z approximately 1*, *ApJ*, **460, L1** (1996).

[6] Madau P., Ferguson H. C., Dickinson M. E., Giavalisco M., Steidel C. C., Fruchter A, *High-redshift galaxies in the Hubble Deep Field: colour selection and star formation history to z 4*, *MNRAS*, **283, 1388** (1996).

[7] Muxlow T. W. B., Richards A. M. S., Garrington S. T., Wilkinson P. N., Anderson B., Richards E. A., Axon D. J., Fomalont E. B., Kellermann K. I., Partridge R. B., Windhorst R. A, *High-resolution studies of radio sources in the Hubble Deep and Flanking Fields*, *MNRAS*, **358, 1159** (2005).

[8] Richards E. A, *The Nature of Radio Emission from Distant Galaxies: The 1.4 GHZ Observations*, *ApJ*, **533, 611** (2000).

[9] Seymour N., McHardy I. M., Gunn K. F, *Radio observations of the 13hXMM-Newton/ROSAT Deep X-ray Survey Area*, *MNRAS*, **352, 131** (2004).

[10] Wilson, G., Cowie, L. L., Barger, A., Burke, D. J, *Star Formation History since* $z = 1.5$ *as Inferred from Rest-Frame Ultraviolet Luminosity Density Evolution*, *AJ*, **124, 1258** (2002).

APPENDIX

Here we present a sample of four sources. Radio contours of MERLIN (left), VLA (right) and combined maps (Centre)overlaid on the optical images in the I band. The contour levels are: 3, 4, 8, 16, 32, 64, 128, 256, 512, 1024 times the noise level: 18 μJy , 12 μJy and 7.5 μJy for MERLIN, combined and VLA respectively. The red and green boxes represents the MERLIN and Combined maps respectively.